Available online at www.sciencedirect.com
SCIENCE DIRECT®
Composites: Part A 35 (2004) 1277–1284
composites
Part A: applied science and manufacturing
www.elsevier.com/locate/compositesa

Monte-Carlo simulation for the fracture process and energy release rate of unidirectional carbon fiber-reinforced polymers at different temperatures

Xianfeng Wang, Martin Y.M. Chiang*, Chad R. Snyder

Polymers Division, US Department of Commerce, National Institute of Standards and Technology, Stop 8544, Gaithersburg MD 20899, USA

Received 13 June 2003; revised 30 March 2004; accepted 6 April 2004

Abstract

This paper presents an analytical approach that combines the modified shear-lag model and the Monte-Carlo simulation technique to simulate the fracture behavior, including the failure process and energy release rate, for unidirectional fiber-reinforced composites with an initial crack at different temperatures. The simulated results, based on a unidirectional carbon fiber-reinforced polymeric (CFRP) composite, were compared with existing experimental observations and measurements. Good agreement exists between the simulation and experimental results. It is found that the critical energy release rate of the unidirectional CFRP composite increases with a decrease in temperature. This increase is primarily due to the temperature-dependence of the composite constituents rather than the residual stresses caused by the change in temperature.

Keywords: A.Polymer-matrix composites (PMCs); B. Fracture toughness; B. Residual/internal stress; C. Statistical properties/methods; Monte-Carlo simuation

1. Introduction

Fiber-reinforced polymer (FRP) composites have been widely used for various kinds of structures in many applications. For composites, a complete and accurate understanding of their failure properties becomes important in approaching the design requirements or in developing new materials. To date, examinations of composite failure behavior have mainly focused on experimental studies [1,2]; therefore, if a change in the composite design parameters is required, a high cost for time and materials is incurred. In this study, a numerical simulation with predictive capability is proposed to obtain fracture properties of composites at different temperatures. The study is limited to the investigation of the tensile fracture properties of unidirectional FRP composites. In most cases, a unidirectional FRP composite layer is the basic constituent of composite structures, and generally its tensile fracture dominates the failure of composites, especially in the cryogenic environments of aerospace and superconductor applications [3].

Among existing micro-mechanical simulation techniques for predicting the tensile failure process and strength of unidirectional FRP composites [4–7], the Monte-Carlo simulation technique coupled with the classical shear-lag model has proven to be very fruitful [7,8]. In the classical shear-lag model, the matrix is assumed to transfer the interfacial shear stress only and not to undertake tensile load (i.e. the tensile breaking of matrix cannot be simulated in the analysis). This assumption is appropriate only if the modulus and strength of the matrix are far lower than that of the fiber (i.e. insignificant tensile stress and strength of matrix). Also, in the model, the matrix is treated as the interface between fibers. As a result, the shear strength of the interface is assumed to be the same as that of matrix. Several researchers [9,10] developed a modified shear-lag model that contains tensile as well as shear deformation for both fiber and matrix in the Monte-Carlo simulation for composites, having comparable matrix and fiber moduli (metal-based composites), to predict their tensile strengths.

In this study, the Monte-Carlo simulation technique with the modified shear-lag model is extended to incorporate the residual stresses, which are induced in the fiber and the matrix due to the mismatch of the coefficient of thermal

* Corresponding author. Tel.: +1-301-975-5186.
E-mail address: martin.chiang@nist.gov (M.Y.M. Chiang).

1359-835X/$ - see front matter © 2004 Elsevier Ltd. All rights reserved.
doi:10.1016/j.compositesa.2004.04.005

expansion (CTE). These residual stresses are more pronounced, especially, for carbon fiber-reinforced polymeric (CFRP) composites since the fiber has negative CTE along its longitudinal direction. In a cryogenic environment, the residual stress in the matrix is tensile. Also, the tensile strength of polymer matrix increases as the temperature decreases [11]. Thus, in order to take into account the stress state and the tensile strength of the matrix, we used the modified shear-lag model in the simulation to predict the fracture behavior of a unidirectional CFRP composite with an edge crack (which mimics a flaw in composites) at room temperature and at cryogenic temperatures. Fracture toughness of the CFRP is predicted in terms of the energy release rate and compared with existing experimental results. Essential details in Monte-Carlo simulation and the calculation of the energy release rate from the simulation will be described in Section 2. Validation of the simulation as well as numerical results and discussion will be presented in Section 3.

2. Monte-Carlo simulation and the calculation of energy release rate

A two-dimensional schematic of a unidirectional FRP with an edge crack for Monte-Carlo simulation is shown in Fig. 1. The composite was under a tensile deformation (v_0) at the far-field and subjected to a change in temperature (ΔT) from room temperature, which was assumed to be stress-free state with respect to thermal stresses. In the simulation, the composite is composed of m strips of the fiber and $m-1$ strips of the matrix with length L (total strips: $2m-1$). Also, the fibers and matrix are divided into $n-1$ segments of length Δx along the fiber direction. As shown in Fig. 1, an edge crack is in the middle of the composite specimen. According to the modified shear-lag model [9], both fiber and matrix are considered to carry

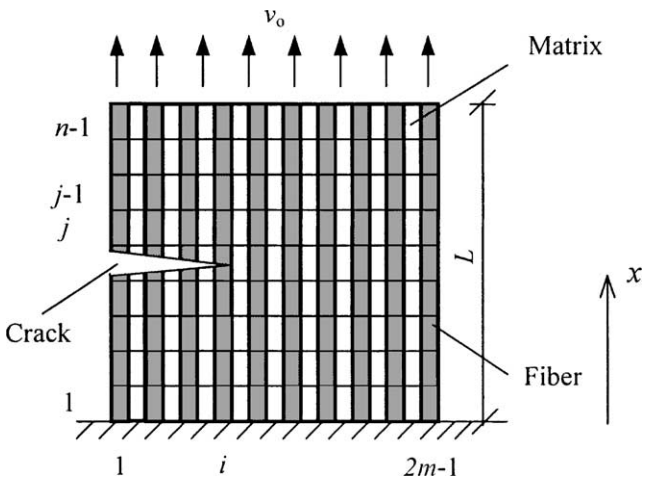

Fig. 1. Two-dimensional schematic of unidirectional composites for Monte-Carlo simulation.

axial stress as well as shear stress. Fig. 2(a) displays the representative segments of Fig. 1 used for the simulation. Here, v is the displacement at the centerline of the fiber or matrix strips. Fig. 2(b) gives the free body diagram of stress distribution for each individual fiber and matrix segment. The normal stresses in the fibers or matrix are denoted by σ. The interfacial shear stress between the fiber and matrix is denoted by τ. It is assumed that the fiber and matrix are linearly elastic and homogeneous materials. Considering the equilibrium of each segment, one can obtain the governing equations expressed in the following form [12]

$$\frac{d^2 v_{(i,j)}}{dx^2} + S_{(i,j)} = 0 \tag{1}$$

with

$$S_{(i,j)} = \frac{h}{E_{(i,j)}A_{(i,j)}}(\tau_{(i,j)} - \tau_{(i-1,j)}) \tag{2}$$

where the subscripts (i,j) indicate the jth segment of the ith strip. i is equal to $1,3,\ldots,2m-l$ for fiber segments and $2,4,\ldots,2m-2$ for matrix segments; j is equal to $1,2,\ldots,n$. A and E are the cross-sectional area and Young's modulus of the segment, respectively. h is the thickness of the unidirectional composites. The boundary conditions in the simulation are

$$v(0) = 0 \qquad \text{and} \qquad v(L) = v_0 \tag{3}$$

where v_0 is the displacement applied at the end of the composite. At the crack surface ($x = L/2$), the boundary condition is

$$\frac{dv_{(i,j)}}{dx} = 0 \qquad (i = 1,2,\ldots k) \tag{4}$$

where k is the number of fiber and matrix segments associated with the crack surface.

At a given temperature, the strength of the matrix and the interfacial strength between the fiber and matrix are assumed to be constant. However, the fiber strength is described statistically by the two-parameter Weibull distribution [6]

$$F(X) = 1 - \exp\left\{-\frac{l}{l_0}\left(\frac{X}{\sigma_0}\right)^{\beta}\right\} \tag{5}$$

where $F(X)$ is the probability that the fiber strength less than or equal to X; σ_0 and β are the Weibull scale and shape parameters, respectively. Note that l_0 is the original gage length at which the single filament tension test and estimation of Weibull parameters are conducted (usually considered as the unit length). l is the extrapolated fiber length of interest. In this study, the length l is taken as the segment length (Δx) used in the simulation, and l_0 is taken as 20 mm.

In the simulation, it is assumed that a constant friction force (τ_c) exists at the interface when debonding occurs

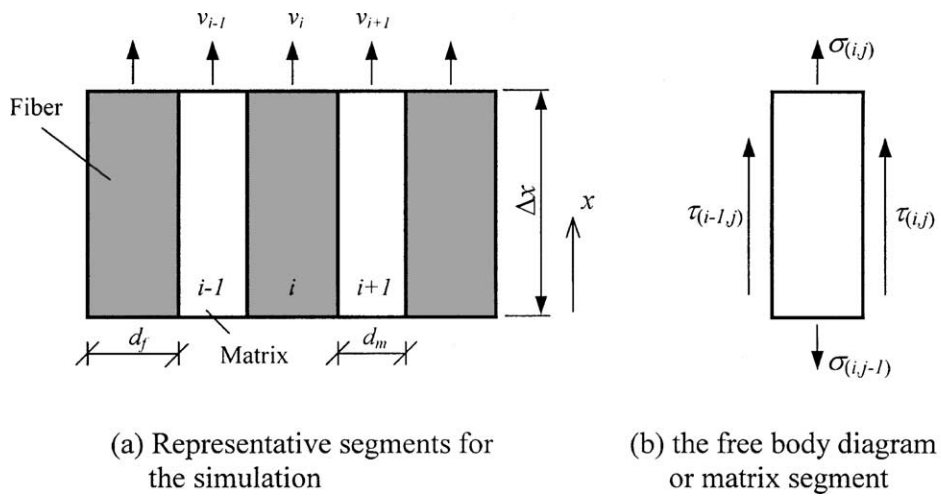

Fig. 2. Representative segments and free body diagram. (a) Representative segments for the simulation. (b) The free body diagram of fiber or matrix segment.

between the matrix and fiber. Also, it is assumed that the $\tau_c = \tau_{max}/2$, where τ_{max} is the interfacial shear strength [8]. Therefore, the interfacial shear stress (τ_i) is as follows

$$\tau_i = \begin{cases} \dfrac{2G_m}{d_m}(v_{(i+1,j)} - v_{(i,j)}) & \text{bonded interface} \\ \tau_c & \text{unbonded interface} \end{cases} \quad (6)$$

where G_m is the shear modulus of matrix, d_m is the distance between the adjacent fibers.

By solving Eq. (1) using the finite difference method for the segment (i,j) with appropriate boundary conditions, one can obtain the displacement of the segment, $v_{(i,j)}$, as follows [12]

$$v_{(i,j)} = \frac{1}{c_1 + c_2 c_3 \Delta x^2}[u_1 + u_2 + c_2 \Delta x^2 (u_3 + u_4)] \quad (7)$$

with

$$c_1 = \begin{cases} H_{i,j+1} + H_{i,j} & j = 1,2,\ldots n-2 \\ H_{i,j} & j = n-1 \end{cases}$$

$$c_2 = \begin{cases} (2 + H_{i,j} + H_{i,j+1})W_{i,j}/4 & j = 1,2,\ldots n-2 \\ (2 + H_{i,j})W_{i,j}/4 & j = n-1 \end{cases}$$

$$c_3 = \begin{cases} P_{i,j} & i = 1 \\ P_{i,j} + P_{i-1,j} & i = 2,3,\ldots 2m-2 \\ P_{i-1,j} & i = 2m-1 \end{cases}$$

$$u_1 = \begin{cases} H_{i,j} v_{i,j-1} & j = 2,3,\ldots n \\ 0 & j = 1 \end{cases}$$

$$u_2 = \begin{cases} H_{i,j+1} v_{i,j+1} & j = 1,2,\ldots n-2 \\ H_{i,j+1} v_0 & j = n-1 \end{cases}$$

$$u_3 = \begin{cases} P_{i,j} v_{i+1,j} + D\tau_c(1 - P_{i,j}) \\ \quad \times \operatorname{sgn}(v_{i+1,j} - v_{i,j})/G_m & i = 1,2,\ldots 2m-2 \\ 0 & i = 2m-1 \end{cases}$$

$$u_4 = \begin{cases} P_{i-1,j} v_{i-1,j} - D\tau_c(1 - P_{i-1,j}) \\ \quad \times \operatorname{sgn}(v_{i,j} - v_{i-1,j})/G_m & i = 2,\ldots 2m-1 \\ 0 & i = 1 \end{cases}$$

where

$$H_{i,j} = \begin{cases} 0 & (X_{i,j} \le \sigma_{i,j}) \\ 1 & (X_{i,j} > \sigma_{i,j}) \end{cases}$$

$$P_{i,j} = \begin{cases} 0 & (\tau_m \le |\tau_{i,j}|) \\ 1 & (\tau_m > |\tau_{i,j}|) \end{cases}$$

$$\operatorname{sgn}(\xi) = \begin{cases} 0 & (\xi = 0) \\ 1 & (\xi > 0) \\ -1 & (\xi < 0) \end{cases}$$

and $W_{ij} = (G_m h)/(E_{(ij)} A_{(i,j)} D)$. D is half of the distance between the adjacent fibers ($D = d_m/2$). Subsequently, using the over-relaxation method [13] to solve Eq. (7), the normal stress (σ, in the loading direction) of the segment (i,j) is

$$\sigma_{(i,j)} = E_{(i,j)} \varepsilon_{(i,j)} \quad (8a)$$

with the corresponding strain $\varepsilon_{(i,j)}$ as

$$\varepsilon_{(i,j)} = \frac{v_{(i,j)} - v_{(i,j-1)}}{\Delta x} - \alpha_{(i,j)} \Delta T \quad (8b)$$

where E and α are the modulus and CTE of the fiber or matrix segments, respectively.

The interfacial shear stress (τ) of the segment (i,j) is:

$$\tau_{(i,j)} = G_m \frac{v_{(i+1,j)} - v_{(i,j)}}{D} \quad (9)$$

In general, the simulation procedure can be described as follows:

(a) Allocate a strength to each fiber segment
(b) For a displacement v_0 applied at the boundary, the $v_{(i,j)}$ are calculated by the successive over-relaxation algorithm, and the normal and interfacial stresses for each segment are then obtained from Eqs. (8) and (9).
(c) Determine the occurrence of a segment break or interfacial debonding. If no break or debonding occurs, the segment stresses are calculated. Otherwise, the governing equation is solved again taking into account the breakage or debonding. This step is repeated until no new breakage occurs.
(d) By increasing the value of v_0 and repeating steps (b) and (c), an apparent stress/strain curve up to composite failure is constructed, and the simulation process ends when the stress drops suddenly. The stress is defined as the averaged applied stress and the strain is defined as the ratio of the specimen displacement to its original length.

The energy required for a unit area of crack growth (G, energy release rate) in a cracked plate, with fixed boundary conditions at the ends, subjected to a constant displacement v_0 (Fig. 1) can be written in the following equation

$$G = -\left(\frac{\partial U}{\partial A}\right)\Big|_{v=v_0} = -\frac{U_a - U_b}{\Delta A} \tag{10}$$

where U is the strain energy stored in the plate. The subscript a indicates the state after cracking and the subscript b represents the state before cracking. ΔA is the area associated with the crack extension. In the Monte-Carlo simulation, with the modified shear-lag model for unidirectional FRP, the energy release is due to the failure of fiber (ΔU_f), matrix (ΔU_m) or interface (ΔU_I) during the crack extension, and the total energy release of the composite can be written as follows

$$\begin{aligned} U_a - U_b &= \Delta U_f + \Delta U_m + \Delta U_I \\ &= \frac{\Delta x}{2}\left(\sum_{i=1}^{N_f} A_f(\sigma_{fa}^i \varepsilon_{fa}^i - \sigma_{fb}^i \varepsilon_{fb}^i) \right. \\ &\quad \left. + \sum_{j=1}^{N_m} A_m(\sigma_{ma}^j \varepsilon_{ma}^j - \sigma_{mb}^j \varepsilon_{mb}^j)\right) - 2N_I h\gamma\Delta x \end{aligned} \tag{11}$$

and

$$\Delta A = n_f A_f + n_m A_m \tag{12}$$

where N_f and N_m are the total number of segments of fibers and matrix in the simulation, respectively. n_f and n_m are the number of failed segments of fibers and matrix, respectively. N_I is the number of interfacial failures between the fiber and matrix segments. γ is the surface energy density of the interface. N_f and N_m should be large enough to make the simulation more representative for the statistical distribution of fiber strength. Here, the values for N_f and N_m were chosen to be 30 according to our numerical experiment. Also, in our simulated results presented later in the paper, it is found that ΔU_I is much smaller than ΔU_f and ΔU_m for the jagged nature of crack growth in a composite. And the results would not make any significant difference with or without the contribution of ΔU_I in Eq. (11). Substituting Eqs. (11) and (12) into Eq. (10), the energy release rate can be rewritten as the following form:

$$\begin{aligned} G = \Delta x\left[\frac{1}{2}\left(\sum_{i=1}^{N_f} A_f(\sigma_{fa}^i \varepsilon_{fa}^i - \sigma_{fb}^i \varepsilon_{fb}^i)\right.\right. \\ \left.\left. + \frac{1}{2}\sum_{j=1}^{N_m} A_m(\sigma_{ma}^j \varepsilon_{ma}^j - \sigma_{mb}^j \varepsilon_{mb}^j)\right) - 2N_I h\gamma\right] / (n_f A_f + n_m A_m) \end{aligned} \tag{13}$$

3. Results of numerical simulations and discussion

Two model problems calculating the energy release rate have been solved to validate the Monte-Carlo simulation with the modified shear-lag model. The first problem dealt with the energy release rate of a homogeneous plate, and the second problem considered a FRP composite plate. The simulated results were compared with existing analytical solutions for validation. Afterwards, the validated simulation was used to obtain the energy release rates for CFRP plate with an edge or center cracks under tensile deformation (Fig. 3) at room or cryogenic temperatures, and the results were compared with existing experimental measurements.

3.1. Validation of the simulation

As shown in Fig. 3(a), a homogeneous plate with a crack embedded in the center and under a remote tensile

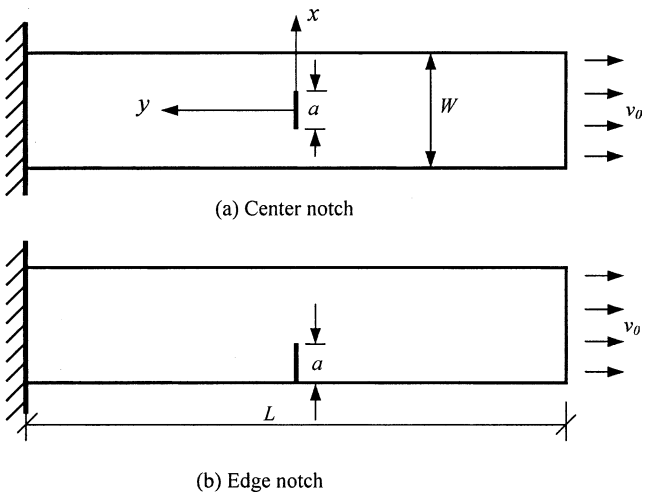

Fig. 3. Sample for simulation and experiment with center and edge notch. (a) Center notch. (b) Edge notch.

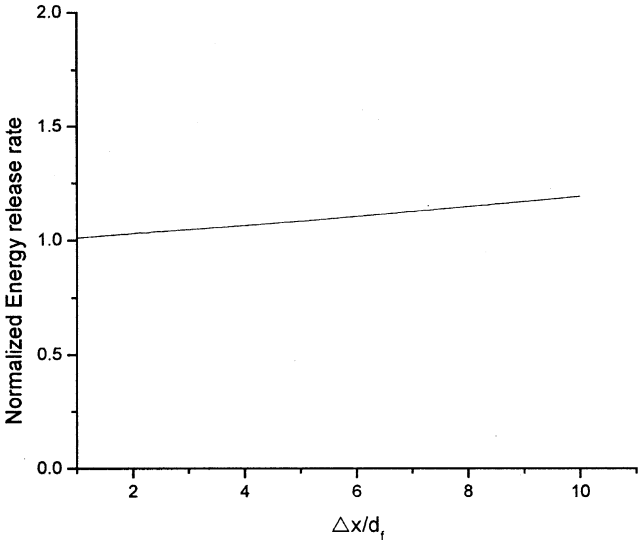

Fig. 4. The relation of simulated normalized critical energy release rate G with the length of segment Δx.

Table 1
Parameters used in the present simulation

Material parameters	296 K		77 K	
	Carbon	Epoxy	Carbon	Epoxy
Elastic modulus, E (GPa)	230	3.2	230	6
Failure strain, ε_m (%)	–	6	–	4
Interfacial shear strength, τ_{max} (MPa)	59.5	–	150	–
Slide friction of interface, τ_c (MPa)	29.75	–	75	–
Weibull shape parameter, β	6.13	–	6.13	–
Weibull scale parameter, σ_0 (MPa)	4134	–	4658	–
Shear modulus of matrix, G_m (MPa)	–	1130	–	2119
Coefficient of thermal expansion along fiber direction, α_L (10^{-6} K^{-1})	−1.1	48	−1.1	48
Cross-sectional area of fiber, A_f (μm^2)	38.46	–	38.46	–
Volume fraction of fiber, V_f (%)	55	–	55	–
Thickness of composite plate, h (μm)	6.2	–	6.2	–
Density of surface energy of interface, γ (J/m^2)	61		61	–

deformation was simulated for the crack extension. For this simulation, the properties of segments associated with the fiber and matrix were assigned to be identical to mimic a homogeneous plate. The initial crack length a is 0.12 mm, and the width of the plate (W) is 1.2 mm. Fig. 4 shows the energy release rate obtained from the simulation, which is normalized by the analytical solutions, as a function of segment length (Δx). It is found that the simulated results approach the theoretical results as Δx decreases, because the numerical error due to the finite difference form associated with Eq. (1) depends on the value of Δx. However, for composite materials, the segment size, Δx, was usually chosen as the ineffective length of the fiber (the length over which the fiber longitudinal stress recovers from zero at a fiber breakage point to the applied stress [14]). This length depends on the mechanical properties of the fiber and matrix. Usually, the value of Δx has been suggested to be (6–10) d_f (fiber diameter) [14,15]. Also, in the simulation, rational numbers of m and n should be chosen according to the accuracy of the result and the consumed time of the simulation. It is found that with the increase in the magnitude of m and n, the simulated results approach to a stationary value. Therefore, in this study, m, n and Δx were chosen as (100, 100 and 10) d_f, respectively.

In the second example, a unidirectional FRP plate with an initial crack embedded in the center was simulated for crack extension (shown in Fig. 3(a)). Assuming perfect bonding between the fibers and matrix and neglecting the yield and failure in the matrix, the fiber strength becomes the only relevant parameter and the crack will propagate along the initial crack plane. The energy release rate (G) can be written in the following form [6]

$$G \approx \frac{\pi}{4}(M+1)V_f\sigma^2\sqrt{\frac{d_m A_f}{E_f G_m h}} \quad (14)$$

where M is the number of broken fibers at the initial crack, V_f is the fiber volume fraction, σ is the far-field stress applied on the plate, d_m is the distance between the adjacent fibers, and G_m is the shear modulus of the matrix. The energy release rate calculated from the simulation is 1.03 times the value calculated using Eq. (14), with M set to 40, and the other needed parameters are inserted from Table 1. Based on these comparisons, the simulation procedure developed in this study is concluded to be valid.

3.2. Numerical simulations of fracture behavior for unidirectional CFRP

Table 1 lists material parameters used for the unidirectional CFRP plate in simulating the energy release rate [16–20]. Fig. 5(a) shows the simulated apparent stress–strain relationships for the CFRP plate with an edge crack (Fig. 3(b)) under tensile deformation at different temperatures. Fig. 5(b) presents the relationships obtained from an experimental measurement [21]. The simulated results have good agreement with the experimental measurements for specimens at temperatures of 77 and 296 K. Both the simulated and experimental results indicate that the slope of the apparent stress–strain curve at 77 K is larger than the one at 296 K, and the relationships are all linear. Fig. 6 presents the simulated failure process (crack extension) of the plate. The simulated failure process starts with the rebounding at the interface along the fiber direction at the crack tip as shown in Fig. 6(a), and then the break occurs at the weakest fiber segment. Subsequently, the matrix breaks, and the interfacial debonding occurs near the breakpoint of the broken fiber. By increasing the loading (deformation), more break events in the fibers, matrix and the interface occur as shown in Fig. 6(b). With further loading,

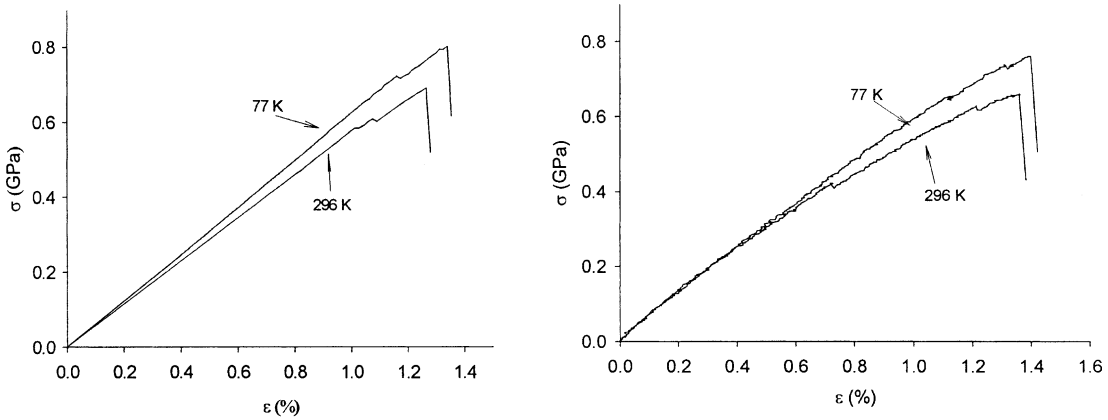

Fig. 5. Apparent stress/strain curve for carbon/epoxy unidirectional composite with edge notch at 296 and 77 K ($a/W = 0.5$). (a) Simulated results. (b) Experimental results.

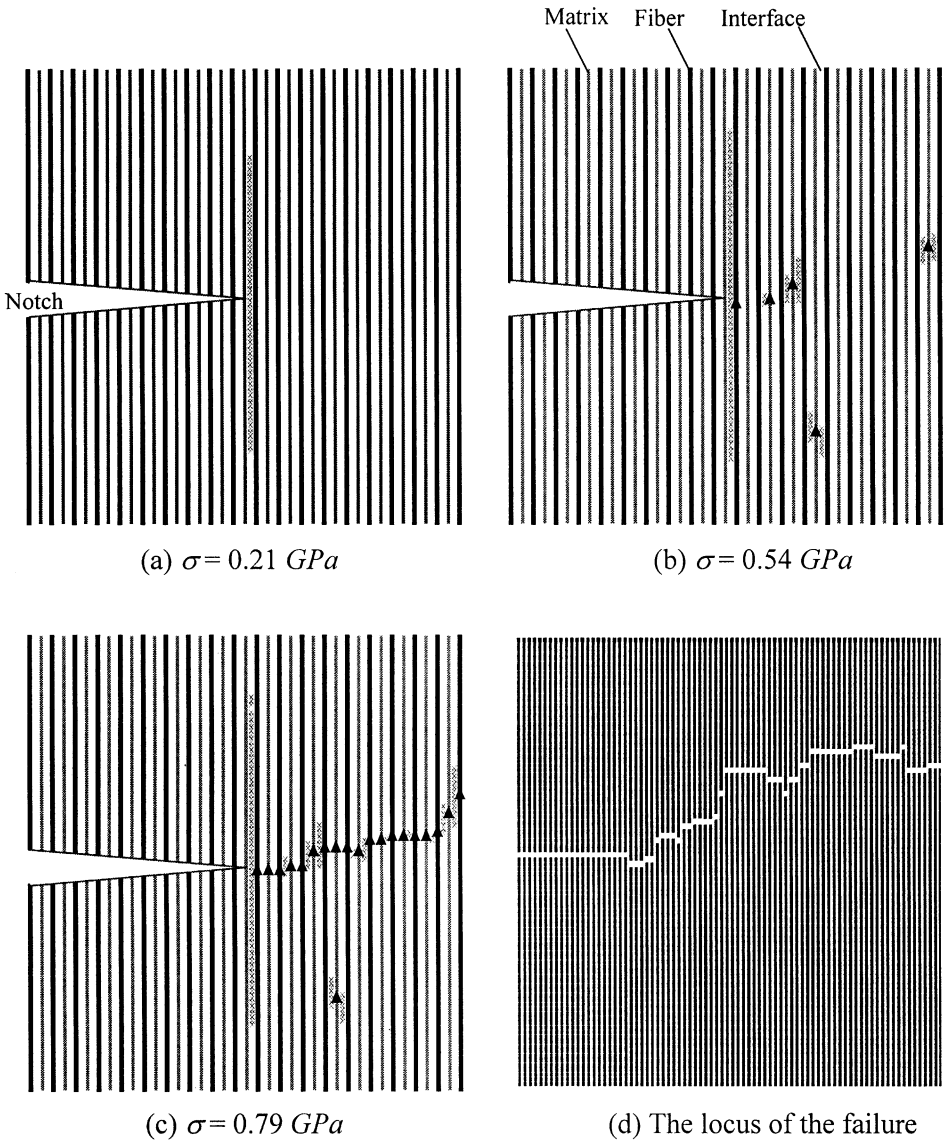

Fig. 6. Fracture process of carbon/epoxy unidirectional composite with edge notch at 77 K. (▲, breakage of fiber and matrix; ×, debondings of interface). Diagrams (a)–(c) are at higher magnification than diagram (d). (a) $\sigma = 0.21$ GPa. (b) $\sigma = 0.54$ GPa. (c) $\sigma = 0.79$ GPa. (d) The locus of the failure.

the failure process progresses (Fig. 6(c)) and leads to the final rupture of the plate as shown in Fig. 6(d). Generally, for unidirectional FRP composites, the energy release rate was calculated under the assumption that the crack extension was along the notch plane, such as the shear-lag model [6] and the Zeweben model [22]. However, from the simulated results (Fig. 6) and experimental observations [21], it is found that the locus of failure has a jagged appearance and the crack does not extend along the notch plane. These random and irregular crack extensions can be attributed to the statistical distribution of fiber strength. Fig. 7 presents the variation of energy release rate, G, with the crack extension obtained from the simulation shown in Fig. 6(d). The solid line is a curve fitting of the energy release rates corresponding to the crack extensions up to 65 μm. By extrapolating the line to the point having the initial crack length (no crack extension), one obtains the critical energy release rate (G_c) of 3.22 kJ/m^2.

Fig. 8 presents the comparisons of work of fracture obtained from the simulation with the experimental observations [21] for the unidirectional CFRP plate with different initial crack lengths (edge crack) at 77 and 296 K. The work of fracture (γ) is defined as the total energy per unit fracture area, where $\gamma = (\sigma_{max}\varepsilon_{max}A_{total}L)/(4A_{crack})$. σ_{max} is the maximum apparent tensile stress applied on the specimen and ε_{max} is the corresponding strain. A_{total} is the total cross-sectional area of the specimen and A_{crack} is the fractured area of the specimen. One can see from Fig. 8 that within the uncertainty good agreement exists between the simulation and the experimental results for the initial crack lengths studied (the uncertainty due to different random distributions of fiber strength is less than 0.5%). Also, both the experimental and simulation results indicate that the fracture work of the CFRP plate increases with a decrease in temperature. Fig. 9 presents the variation of the simulated

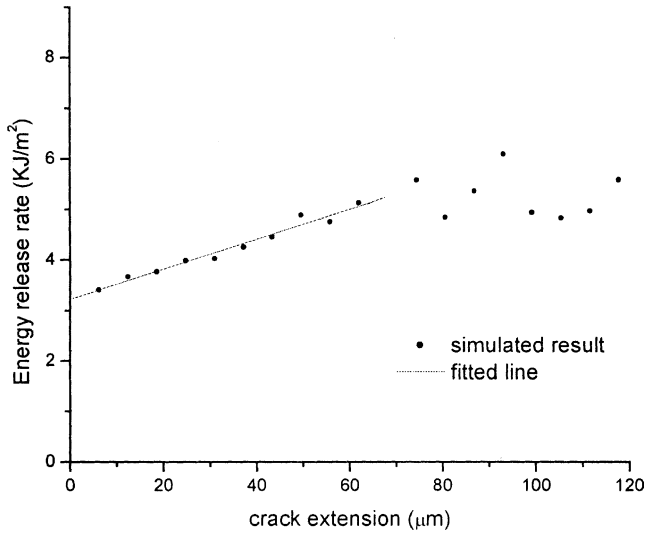

Fig. 7. Simulated relation of energy release rate G with the crack extension.

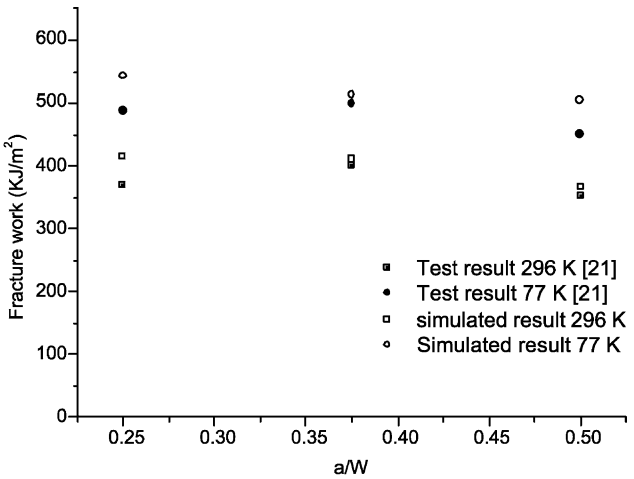

Fig. 8. The simulated and tested fracture work of unidirectional CFRP with different initial crack length at 77 and 296 K ($V_f = 0.55$).

G_c of the plate as a function of initial crack length. As expected, from Fig. 9, G_c is found to be independent of the initial crack length. Also, the G_c increases at 77 K by 23% relative to the G_c at 296 K. The increase of the G_c at low temperature can be attributed to the temperature-dependent constituent properties and the residual stresses caused by the change in temperature. By a separate study in the simulation, two attributes were independently considered. It is found that the residual stresses are not essential causes for the trending upward of the G_c at low temperature. The temperature-dependence of σ_0 (Weibull scale parameter, Eq. (5)) and the interfacial shear strength are the dominant factors in the increase of the energy release rate at low temperatures.

Finally, it is worthwhile to examine the validity of Eq. (14) for evaluating the G_c of unidirectional fiber-reinforced composite. Fig. 10 displays the G_c obtained from Eq. (14) and the simulation as a function of Weibull shape parameter (β). As indicated in Fig. 10 one can see that, when $\beta \geq 20$,

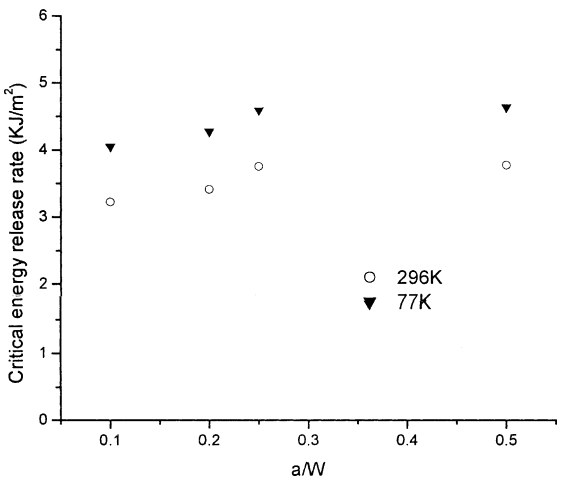

Fig. 9. The simulated critical energy release rates of unidirectional CFRP with different initial crack length at 77 and 296 K ($V_f = 0.55$).

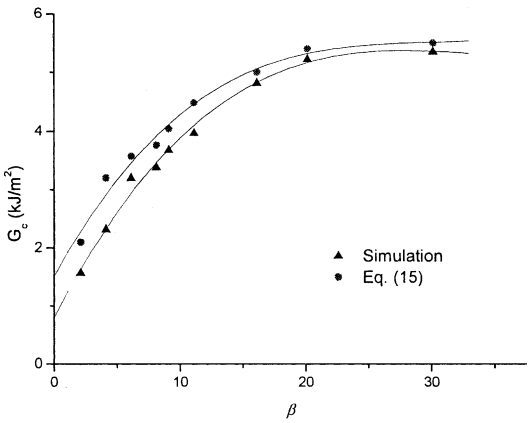

Fig. 10. The energy release rate (G_c) evaluated from Eq. (14) and the simulation as a function of Weibull shape parameter (β). The solid lines are obtained from curve fittings of data.

the values of G_c become steady state and Eq. (14) would be much closer to the true situation (simulation).

4. Conclusion

By coupling the Monte-Carlo simulation with the modified shear-lag, model, a simulation procedure with an analytical method has been developed in this study to predict the failure process including the fiber breaking, matrix cracking and interfacial debounding. The simulation can predict the critical energy release rate (or the fracture work) for the unidirectional CFRP composites at different temperatures. Also, the proposed procedure could be applied to any unidirectional fiber-reinforced composite. The simulated results showed a good agreement with the experimental data for the stress–strain relation and energy release rate of unidirectional CFRP composites. More importantly, the critical energy release rate of the unidirectional CFRP composite, which is relevant to the fracture toughness, increases with a decrease in temperature. This increase is primarily due to the temperature-dependence of the composite constituents rather than the residual stresses induced due to the change in temperature.

References

[1] Reed RP, Golda M. Cryogenic properties of unidirectional composites. Cryogenics 1994;34:908–28.
[2] Reed RP, Golda M. Cryogenic composite support: a review of strap and strut properties. Cryogenics 1997;37:233–50.
[3] Schutz JB. Properties of composite materials for cryogenic applications. Cryogenics 1998;38:3–12.
[4] Zhou SJ, Curtin WA. Failure of fiber composites: a lattice green function model. Acta Metall Mater 1995;43:3093–104.
[5] Lienkamp M, Exner HE. Prediction of the strength distribution for unidirectional fiber reinforced composites. Acta Mater 1996;44: 4433–46.
[6] Beyerlein IJ, Phoenix SL. Statistics of fracture for an elastic notched composite lamina containing Weibull fiber. Part 1. Features from Monte-Carlo simulation. Eng Fract Mech 1997;57:241–65.
[7] Kong POH. A Monte-Carlo study of the strength of unidirectional fiber-reinforced composites. J Compos Mater 1979;13:311–27.
[8] Goda K, Leigh PS. Reliability approach to the tensile strength of unidirectional CFRP composite by Monte-Carlo simulation in a shear-lag model. Compos Sci Technol 1994;50:457–68.
[9] Ochiai S, Hojo M. Stress disturbances arising from cut fiber and matrix in unidirectional metal matrix composites calculated by means of a modified shear lag analysis. J Mater Sci 1996;31: 3861–9.
[10] Nairn JA, Mendels DA. On the use of planar shear-lag methods for stress-transfer analysis of multilayered composites. Mech Mater 2001; 33:335–62.
[11] Fitzer E, Weiss R. Processing and uses of carbon fiber reinforced plastics. Dusseldorf: VDI-Verlag; 1981. p. 45.
[12] Wang XF, Zhao JH. Monte-Carlo simulation to the tensile mechanical behavior of unidirectional composites at low temperature. Cryogenics 2001;41:683–91.
[13] Ferzigr JH. Numerical methods for engineering application. New York: Wiley; 1981.
[14] Fariborz SJ, Tang CL, Harlow DG. The tensile behavior of intraply hybrid composites. I. Model and simulation. J Compos Mater 1985; 19:334.
[15] Fariborz SJ, Harlow DG. The tensile behavior of intraply hybrid composites. II. Micromechanical model. J Compos Mater 1987;21: 856.
[16] Beaumont PWR. Fiber composite. Chin Acad Sci R Soc Present 1986; .
[17] Hartwig G. Status and future of fiber composites. In: Reed RP, Ficheet FR, editors. Advances in cryogenic engineering (materials), 40B. New York: Plenum Press; 1994. p. 961–75.
[18] Hartwig G, Knaak S. Fiber-epoxy composites at low temperatures. Cryogenics 1984;24:639–47.
[19] Wang XF, Zhao JH, Jiang HY, Gong M. Statistical characteristics of strength at low temperature for glass and carbon fibers. J Inorg Mater 2003;18:45–9.
[20] Tsai SW, Hahn HT. Introduction to composite material. New York: Technomic Publishing; 1980.
[21] Wang XF, Gong M, Wu XP, Zhao JH. Experimental study on mechanical behavior of laminates at low temperature. Cryogenics 2004; in press.
[22] Zweben C. Analysis of the test methods for high modulus fibers and composites. ASTM STP 521 1973;65–73.